CHAPTER FOUR

Structure and correlations for harmonically confined charges

Jeffrey Wrighton and James Dufty*
Department of Physics, University of Florida, Gainesville, FL, United States
*Corresponding author: e-mail address: dufty@phys.ufl.edu

Contents

1. Introduction 40
2. Density functional theory 42
3. Classical mechanics 43
   3.1 Fluid phase 44
   3.2 Ordered phase 46
4. Quantum mechanics 51
5. Discussion 52
Acknowledgments 53
References 53

Abstract

Coulomb charges confined by a harmonic potential display a rich structure at strong coupling, both classical and quantum. A simple density functional theory is reviewed showing the essential role of correlations in forming shell structure and order within the shells. An overview of previous comparisons with molecular dynamics and Monte Carlo simulations is summarized and extended. It is shown that correlations for the fluid phase (shell structure only) are well approximated by those for the uniform one-component plasma even at very strong coupling. A corresponding representation of the correlations for the ordered phase is still an open question. The confirmed success for the classical density functional theory is important for the subsequent representation of the quantum case. Here, a mapping of the quantum description onto an equivalent classical description with effective potentials allows direct application of the classical methods, both theory and simulation. This is particularly relevant at low but finite temperatures where quantum simulation methods are compromised. The special case of Coulomb charges in a harmonic trap is the simplest example of more complex systems of experimental interest where confinement and strong coupling play an essential role (e.g., quantum dots, ions in complex traps, electrons on a helium surface, dusty Yukawa plasmas, ultracold neutral plasmas).

Advances in Quantum Chemistry, Volume 85
ISSN 0065-3276
https://doi.org/10.1016/bs.aiq.2022.04.003

1. Introduction

The problem considered here is the structure and correlation among N equal Coulomb charges confined by an external harmonic potential. It is a generalization of the Thomson problem[1] for charges confined to the surface of a sphere, posed 117 years ago, to three dimensions and finite temperatures. The ground state for the harmonic confinement is well studied, exposing a rich shell structure (distribution of particles localized about well-defined radii with localization on each radius similar to those of the single sphere Thomson problem). Within classical mechanics, these ground-state results have been quantified in detail via shell models, molecular dynamics (MD) simulation, and Monte Carlo (MC) simulation.[2–7] They are also realized experimentally for dusty plasmas. The corresponding results for confined charges at finite temperatures are the extension described here. We provide here a summary of our theoretical work in collaboration with the Bonitz group at the Institute fur Theoretische Physik und Astrophysik, Christian-Albrechts Universitat, Kiel.[8–11] In addition, we describe the method for extension to quantum theory and list some remaining outstanding problems.

The primary effect of temperature on the classical ground-state shell models is to broaden the sharp shell structure and smooth their angular distribution due to thermal motion. The governing parameters are the Coulomb coupling constant Γ (ratio of Coulomb to thermal energies of a pair) and the average number of charges $\bar{N}$. The number of shells is fixed by $\bar{N}$, while their relative resolution (sharpness) is determined by Γ. The zero temperature ground-state results from shell models are recovered in the limit of large Γ. A simple approximate density functional theory described below is able to capture these results quantitatively, in comparison with those from MC simulations. It is based on approximating correlations among the charges in the trap by those in the uniform one-component plasma (OCP). The close relationship of correlations in these two quite different systems has been confirmed by MD simulation.[10,11]

At still larger Γ, corresponding to lower temperatures, the rotational invariance of the fluid phase is broken and the particles within each shell become localized about sites close to those of the Thomson problem for a single shell. Those localized domains are approximated here by Gaussian

distributions centered at these sites, and the correlations among them are calculated showing good agreement with results from MC simulation.

The effects studied here result from strong coupling conditions for which there are relatively few theoretical methods available. In the classical case, the density functional model described below is confirmed by MD and MC simulations. The latter simulations are not available for the quantum case, and the quantum density functional model has problems at finite temperatures. However, it has been shown that the quantum system can be mapped onto a corresponding classical system with quantum effects embedded in effective Coulomb and trap potentials.[12] Applications to the OCP (jellium) show good agreement with quantum Monte Carlo results.[13,14] This approach has been applied subsequently to the case of quantum charges in a harmonic trap[15,16] as described below. In this way, a broad scope of confined Coulomb systems of interest can be addressed. Fig. 1 gives a simple overview of the parameter space.

It is a pleasure to dedicate this contribution to our friend and colleague of many years, Professor John (Jack) Sabin. Jack has been an inspiration for all

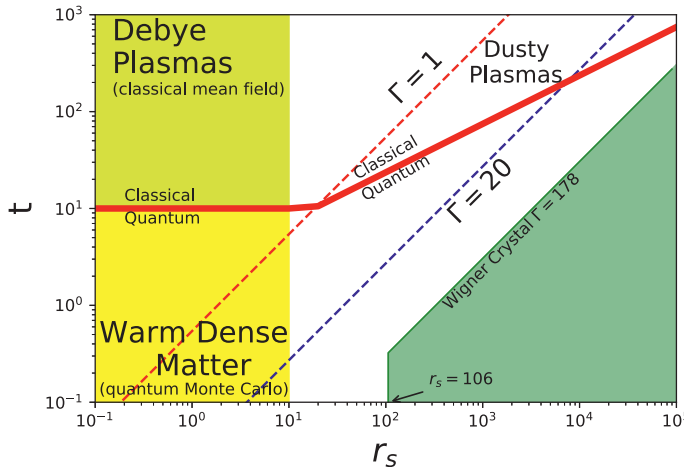

Fig. 1 Overview of the relevant parameter space. Here, r_s is the Wigner–Seitz radius in terms of the Bohr radius of the confined particles ($r_s = r_0/a_b$), and t is the temperature relative to the ideal gas Fermi temperature per particles ($t = k_B T/\varepsilon_F$).[16] Here, $a_b = \hbar^2/me^2$ and $\varepsilon_F = \hbar^2(3\pi^2\bar{n})^{2/3}/2m$, where $\bar{n}$ is the average density from (6). The Fermi energy is used for scaling as it is relevant to the low-temperature quantum domain and thus t is a measure of the onset of quantum effects. Note that the classical phase for dusty plasmas shown in this figure represents the fluid phase.

that is expected of those with an academic career, exemplifying the best in teaching, research, and administration. His cheerful nature and good will have brightened the lives of all who knew him well.

2. Density functional theory

Consider N particles of charge q at equilibrium in a harmonic trap at inverse temperature β. The free energy is denoted $F(\beta|n)$, indicating that it is a function of β and a functional of the nonuniform density $n(\mathbf{r})$. The equilibrium density profile is determined from

$$\frac{\delta F(\beta|n)}{\delta n(\mathbf{r})} = \mu - V(r), \qquad V(r) = \frac{1}{2} m\omega^2 r^2. \tag{1}$$

The potential $V(r)$ is the confining harmonic trap. The free energy functional can be separated into that for a system without interactions, $F_0(\beta|n)$, and a remainder $F_{ex}(\beta|n)$ containing all effects of Coulomb interactions among the particles

$$F(\beta|n) = F_0(\beta|n) \; + \; F_{ex}(\beta|n). \tag{2}$$

A formal representation for the excess free energy in terms of pair correlations can also be written exactly

$$F_{ex}(\beta|n) = -\int_0^1 d\gamma(1-\gamma) \int d\mathbf{r} d\mathbf{r}' n(\mathbf{r}) n(\mathbf{r}') \beta^{-1} c^{(2)}(\mathbf{r}, \mathbf{r}'|\gamma n), \tag{3}$$

where $c^{(2)}(\mathbf{r}, \mathbf{r}'|n)$ is the direct pair correlation function

$$\beta^{-1} c^{(2)}(\mathbf{r}, \mathbf{r}'|n) \equiv -\frac{\delta^2 F_{ex}(\beta|n)}{\delta n(\mathbf{r}) \delta n(\mathbf{r}')}. \tag{4}$$

In this way, Eq. (1) is an equation for the local density in terms of the pair correlations of the direct correlation function[9]

$$\frac{\delta F_0(\beta|n)}{\delta n(\mathbf{r})} = \mu - V(r) \; + \int_0^1 d\gamma \int d\mathbf{r}' n(\mathbf{r}') \beta^{-1} c^{(2)}(\mathbf{r}, \mathbf{r}'; \gamma n). \tag{5}$$

The average density $\bar{n}$ is defined by

$$\bar{n} = \frac{\bar{N}}{V}, \qquad \bar{N} = \int d\mathbf{r} n(\mathbf{r}). \tag{6}$$

The system is self-confined with spherical symmetry. The maximum radius R is the point at which Coulomb repulsion force on a particle is balanced by the harmonic trap confinement

$$\bar{N}\frac{q^2}{R^2} = m\omega^2 R, \qquad V = \frac{4}{3}\pi R^3. \tag{7}$$

The mean distance between particles r_0 is introduced by

$$\frac{4}{3}\bar{n}\pi r_0^3 = 1. \tag{8}$$

Scaling the coordinates with respect to r_0 in the above equations gives the dimensionless form

$$\frac{\delta F_0^*(n^*)}{\delta n^*(\mathbf{r}^*)} = \beta\mu - \frac{1}{2}\Gamma r^{*2} + \int_0^1 d\gamma \int d\mathbf{r}'^* n^*(\mathbf{r}'^*) c^{(2)}(\mathbf{r}^*, \mathbf{r}'^*; \gamma n^*), \tag{9}$$

where

$$F_0^*(n^*) = \beta F_0(\beta|n); \qquad n^*(\mathbf{r}^*) = n(\mathbf{r})r_0^3, \qquad \Gamma = \beta m\omega^2 r_0^2 = \beta\frac{q^2}{r_0}. \tag{10}$$

The parameter Γ is the Coulomb coupling constant (Coulomb energy of a pair at the average distance relative to the thermal energy β^{-1}). The constant $\beta\mu$ can be eliminated in terms of $\bar{N}$.

Up to this point, the results apply for both quantum and classical mechanics. The classical case is considered more explicitly next.

3. Classical mechanics

Within classical statistical mechanics, $F_0(\beta|n)$ can be written exactly as a functional of the density

$$F^{(0)}(\beta|n) = -\frac{1}{\beta}\int d\mathbf{r} n(r)\left(1 - \ln\left(n(r)\lambda^3\right)\right). \tag{11}$$

Here, $\lambda = \left(h^2\beta/2\pi m\right)^{1/2}$. Then Eq. (9) becomes[9]

$$\ln\left(n^*(\mathbf{r}^*)\right) = \ln\left(\left(\frac{\lambda}{r_0}\right)^3 e^{\beta\mu}\right) - \frac{1}{2}\Gamma r^{*2} + \int_0^1 d\gamma \int d\mathbf{r}'^* n^*(\mathbf{r}'^*) c^{(2)}(\mathbf{r}^*, \mathbf{r}'^*; \gamma n^*). \tag{12}$$

The constant first term on the right side can be eliminated in terms of $\bar{N}$. Consequently, the dimensional density profile and associated free energy density profile depend only on the two parameters $\bar{N}$ and Γ.

The solutions to (12) are expected to confirm the following qualitative behavior observed from ground-state energy functions,[8] and MC and MD simulations.[7] For given $\bar{N}$, the profiles have a strong dependence on the coupling strength Γ. At very small values, the density profile is rotationally symmetric and monotonically decreasing to zero from a maximum at $r^* = 0$. At increasing values, the radial dependence develops local maxima, referred to as shells. This is illustrated in Fig. 2. The number of shells increases with $\bar{N}$ and their width sharpens with increasing Γ. The shell populations are greater for increasing radius and grow linearly with $\bar{N}$.

Eventually, at sufficiently large Γ rotational symmetry is broken. The uniform distribution of particles within each shell distorts to local domains for the associated population. Their locations are close to those of the Thomson problem—the ground-state configuration for a given number of charges confined to a sphere. In the following, the extent to which approximations to the density functional theory (12) captures these features is described.

3.1 Fluid phase

The approximate determination of the pair correlations described by the direct correlation functional in (12) is motivated as follows. First, it is shown

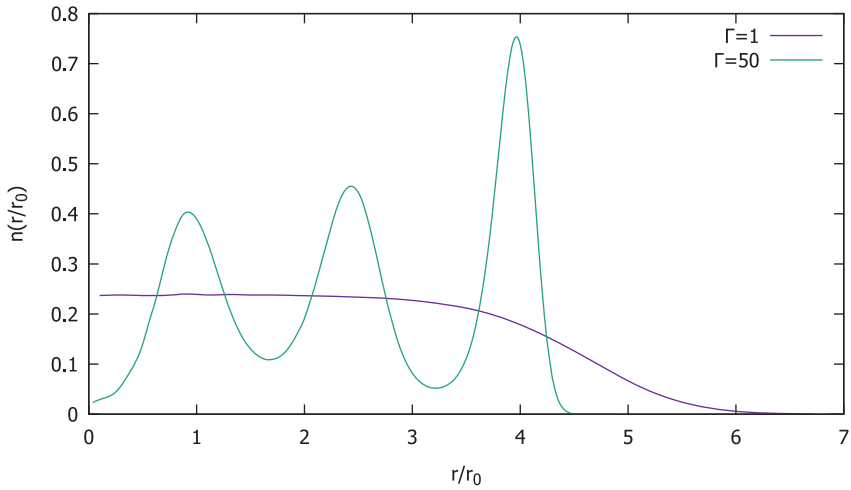

Fig. 2 Formation of shell structure in a harmonic trap as the coupling constant Γ increases. Monte Carlo simulation of 100 particles in a trap.

elsewhere that the functional $F_{ex}(\beta|n)$ is exactly equal to the corresponding system with a uniform neutralizing background (inhomogeneous jellium), i.e., charges in a uniform neutralizing background with the same harmonic potential[17]

$$F_{ex}(\beta|n) = F_{jex}(\beta|n). \tag{13}$$

The advantage of this is that the OCP has a finite uniform limit in the absence of the harmonic confinement, which is the uniform OCP. It has been observed elsewhere[11] that the distribution of pairs within the trap *without reference to their center of mass* position is almost identical to those of the OCP (see Fig. 3). Therefore, as an approximation for the fluid phase, OCP correlations have been used,

$$c^{(2)}(\mathbf{r},\mathbf{r}';\lambda n)\big|_{\lambda n=\overline{n}} = c^{(2)}(\mathbf{r},\mathbf{r}';\overline{n}) = c^{(2)}_{OCP}(|\mathbf{r}-\mathbf{r}'|;\overline{n}). \tag{14}$$

Evaluation of the direct correlation function for the OCP in (14) still poses a formidable many-body problem at strong coupling. However, it is a well-studied problem and an excellent approximation, the *adjusted hypernetted chain approximation* (AHNC), is known.[20,21] The solutions to (12) with these two approximations for $c^{(2)}(\mathbf{r},\mathbf{r}';n)$ give all of the above expected properties for the density profile quantitatively in comparison to MD and MC results, across the entire domain of Γ and $\bar{N}$. An example is illustrated in Fig. 4.

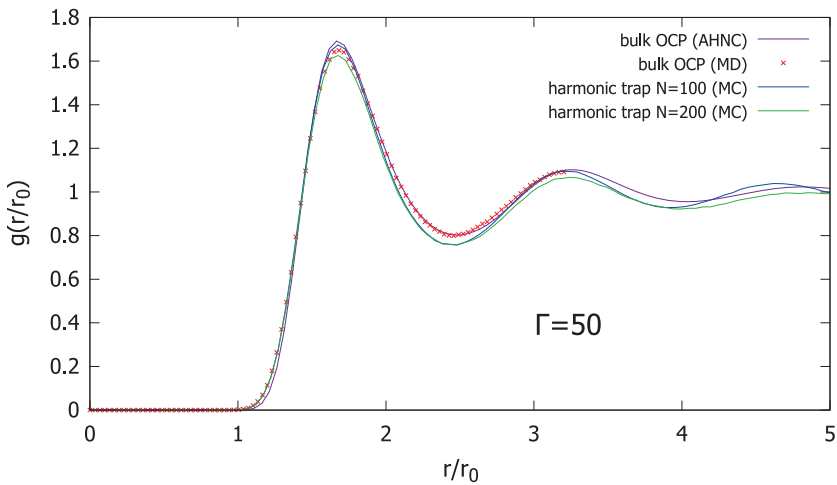

Fig. 3 Comparison of the pair distribution of particles in a one-component plasma (OCP) and harmonic trap. MD calculations for the OCP were performed using Sarkas.[18,19]

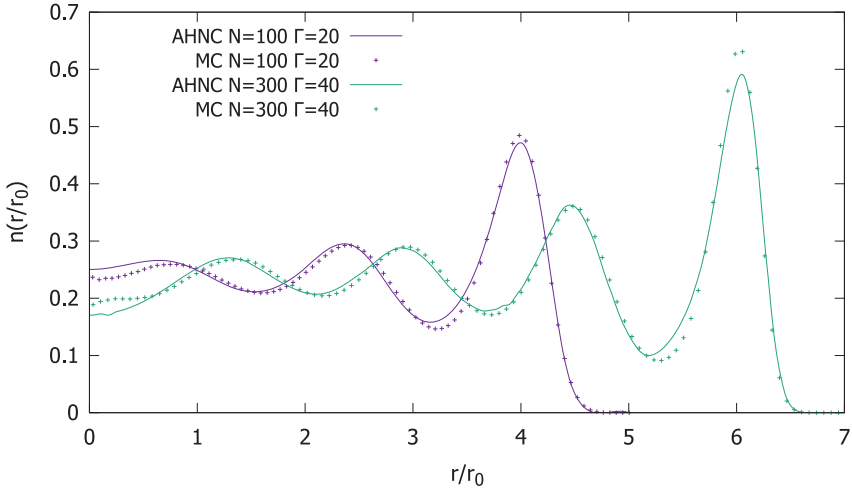

Fig. 4 Comparison of density profiles for AHNC and MC, for $N = 100$ and $\Gamma = 20$, and for $N = 300$ and $\Gamma = 40$.

3.2 Ordered phase

In the fluid phase, the particles are uniformly distributed throughout each shell. As the coupling increases eventually the particles enter an ordered state where rotational symmetry is broken within the shell. Fig. 5 shows the angular correlations within the outer shell from a MD simulation, for three values of the coupling constant corresponding to fluid and ordered phases. The system consisted of $N = 38$ charges, with 32 in the outer shell. The pair correlation function $g(\theta)$ is the probability to find a particle displaced on the shell by an angle θ from an arbitrary reference particle. As in a uniform fluid, the peaks represent nearest neighbor, next nearest neighbor, etc. At the lower values of Γ, there is not much qualitative difference in the angular correlations, but the correlation peaks are narrowing and some structure is starting to develop in the form of shoulders in the middle peaks. For significantly larger values of Γ however, a definite structure appears within each peak of the correlation graph. In particular, the two broad peaks at $\Gamma = 100$ that appeared at 70 and 110 degrees have condensed into triplets at $\Gamma = 1000$. In addition, the two peaks at 40 and 140 degrees are showing the beginning formation of a doublet structure with the presence of shoulders at $\Gamma = 1000$. This set of doublet and triplet features persists at much higher Γ, without the appearance of any more peaks.

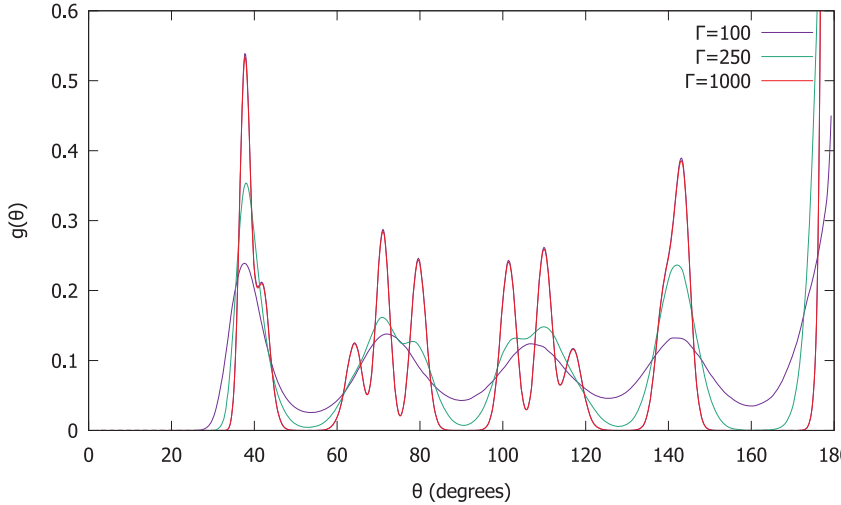

Fig. 5 Angular correlations within a single shell from MD simulation. The harmonic trap contained 38 particles, with 32 in the outer shell. MD simulations were performed with LAMMPS.[22,23]

These features can be modeled using a thin-shell model where the particle configuration results from the Thomson problem.[1] The context of the original Thomson paper lies in a mistaken view of atomic structure at the time it was written, addressing the question of the ground-state energy of charges fixed to a sphere. It is thus related to the questions here of effectively having multiple spheres representing the shell structure and the distribution of charges within those spheres. At very low temperature (large Γ), simulations and other studies show that the density changes from a uniform distribution to have features very close to those of the Thomson problem. As shown below, the number of localized sites and their locations are quite similar. Differences can be associated with the widths of the shells and interactions between different shells. The specific ordering depends on the number of charges because of the spherical geometry. In Fig. 6, the Thomson configuration for a randomly chosen particle from a system containing $N = 32$ charges is shown along with constant-angle planes showing the angular displacement of the other particles. To compare more directly, the angular correlations of all 32 charges in the Thomson problem were calculated. A plot of the angular displacement of all pairs is shown in Fig. 7. The charges occur in two different angular

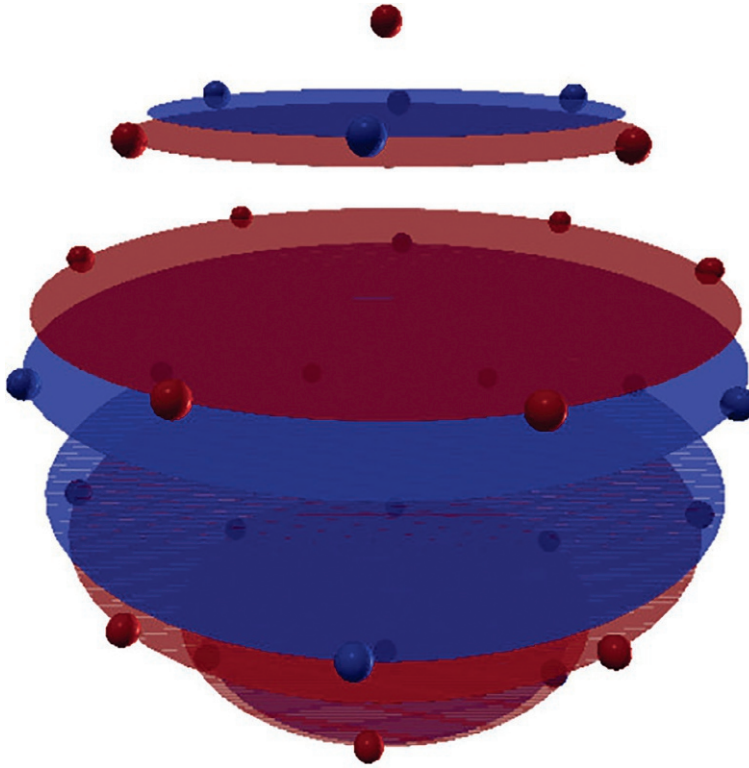

Fig. 6 A system of 32 charges in the Thomson problem. *Horizontal circles* connect those charges that are at constant angle θ from the chosen particle at the *top* of the figure.

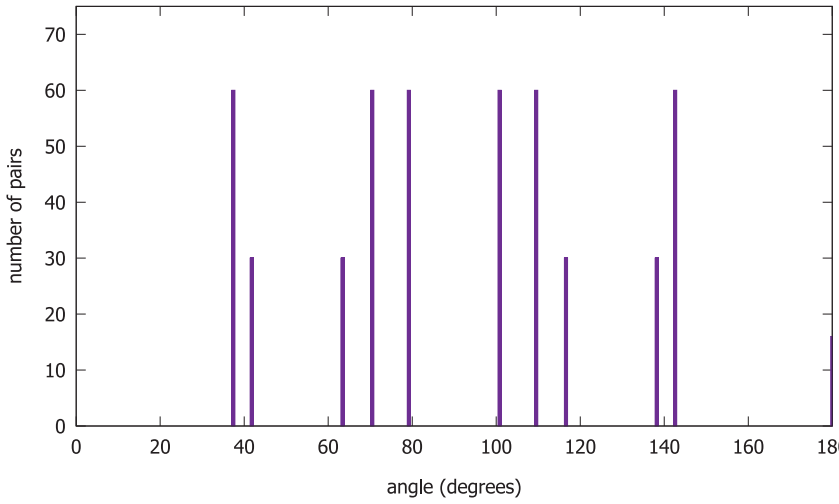

Fig. 7 Number of each angle present between each pair of particles in the Thomson system for $N = 32$ charges.

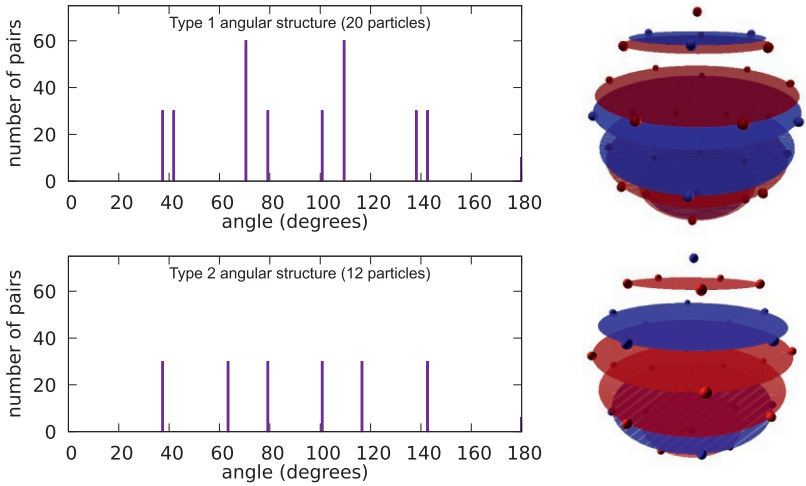

Fig. 8 Angular distribution for the two types of angular configuration for $N = 32$ charges in the Thomson problem. The first type of angular configuration has particles at eight specific angles between $\theta = 0$ degrees and $\theta = 180$ degrees. There are 20 particles in this configuration. The remaining 12 particles are in a configuration with 6 specific angles to the other particles. Plots show the total number of bonds that each population contributes for the entire system; their sum gives the results in Fig. 7.

correlation structures. These are shown in Fig. 8. The combination of these two populations accounts for the specific angular correlation structure for the case of $N = 32$ charges.

To account for thermal effects, the charges were modeled using a Gaussian function along the sphere of the form

$$f(\theta) = \sqrt{\frac{\alpha}{\pi}} \exp\left(-\alpha(\theta - \theta_0)^2\right) \tag{15}$$

where θ_0 is the angle corresponding to the Thomson site and α is a parameter that increases with decreasing temperature. Fig. 9 shows how this model reproduces the correct splitting, from the four broad peaks at small Γ which condense to the characteristic doublets and triplets at higher Γ. Fig. 10 shows the effect of the fitting parameter α showing how it models the effect of thermal motion. This supports the idea of considering the Thomson sites on a sphere to be analogous to a fundamental lattice for the ordered state, to the extent that the shell can be approximated as thin.

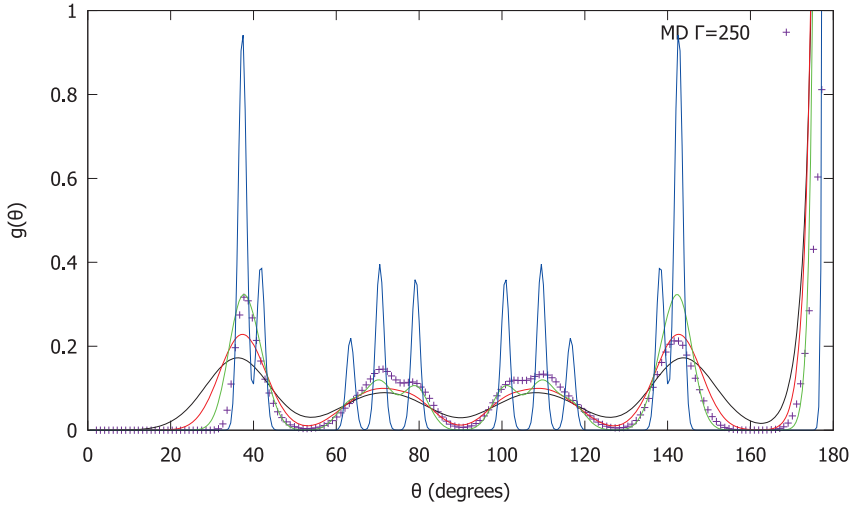

Fig. 9 Solid lines: evolution of the thermally broadened angular correlations from the Thomson problem as the parameter α increases. Peak height increases with larger α. Crosses: comparative results from MD at $\Gamma = 250$.

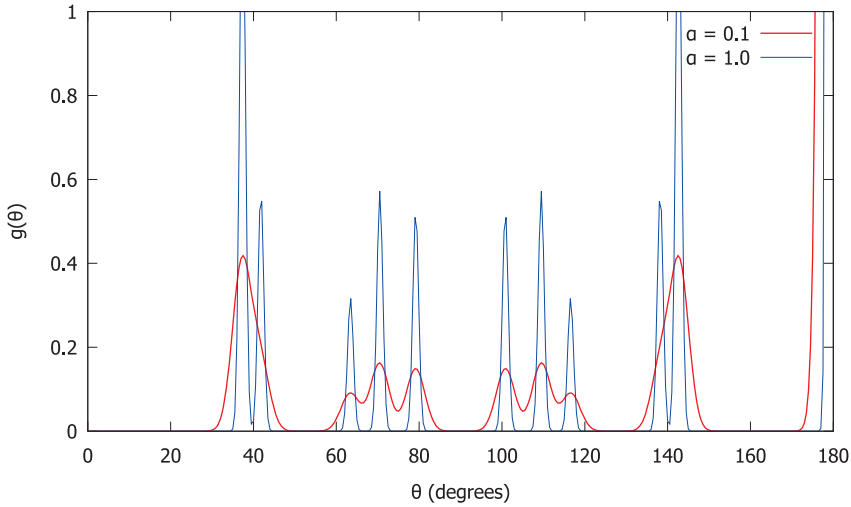

Fig. 10 Angular correlations from the thermally broadened Thomson system for two values of the fitting parameter α. Here, there are $N = 32$ charges in the system. The structure follows the same behavior as MD simulations for 32 particles in a shell.

In principle, the value of α in the ordered phase, for given Γ, $\bar{N}$, should be obtained from minimizing the above free energy functional using the assumed Gaussian density profile. In the fluid phase, the value of α would be large, representing a uniform profile. At very large Γ, approaching the

ground state, the value of α would approach zero. However, the assumption of the Thomson sites should first come from solutions of (12). This could be quite difficult since ground-state studies from simulations suggest there are many metastable configurations as well.

4. Quantum mechanics

The above classical description of confined charges at strong coupling has exploited the methods of density functional theory, liquid state theory, MD, and MC. At low temperatures, at or below the Fermi temperature, quantum effects become important and many of these classical methods do not apply directly. An accurate quantum theory at finite temperatures, strong coupling, and confinement is still a challenging problem. Numerical methods such as quantum Monte Carlo are applicable at zero temperature but become less controlled as the temperature increases, particularly for fermions. A quite different approach is to develop an exact mapping of the quantum equilibrium structure to an effective classical problem. This has been done recently, allowing application of the above classical methods to quantum systems.[12] Structure and correlation calculated in this way for the OCP have shown good accuracy in comparison with recent quantum MC simulations.[13,14]

More recently, the effective classical representation of a system of quantum charges in a harmonic trap has been explored.[15,16] The primary differences from the classical description above are modifications of the Coulomb potential and the trap potential to accommodate quantum effects of diffraction and exchange symmetry. The exchange symmetry implies an additional pair interaction among charges even in the absence of Coulomb interactions. It is repulsive or attractive depending on the quantum statistics (Fermions or Bosons). The other important quantum effects is removal of the short distance Coulomb singularity. A new parameter appears, in addition to Γ and $\bar{N}$, the temperature relative to the Fermi temperature ($t = k_B T/e_F$ where e_F is the ideal gas Fermi energy per particle). For $t \gg 1$, the above description of shell structure and correlations is recovered for strong coupling. At smaller t, the effects of exchange degeneracy are incorporated by imposing the exact noninteracting density profile for the ideal gas. This is nontrivial since the classical representation of the quantum ideal gas has effective interactions. The additional effects of exchange and diffraction are included via the direct correlation function with modified Coulomb interactions. Fig. 11 shows a self-similar change in the classical two-shell structure being compressed due to quantum effects on the harmonic

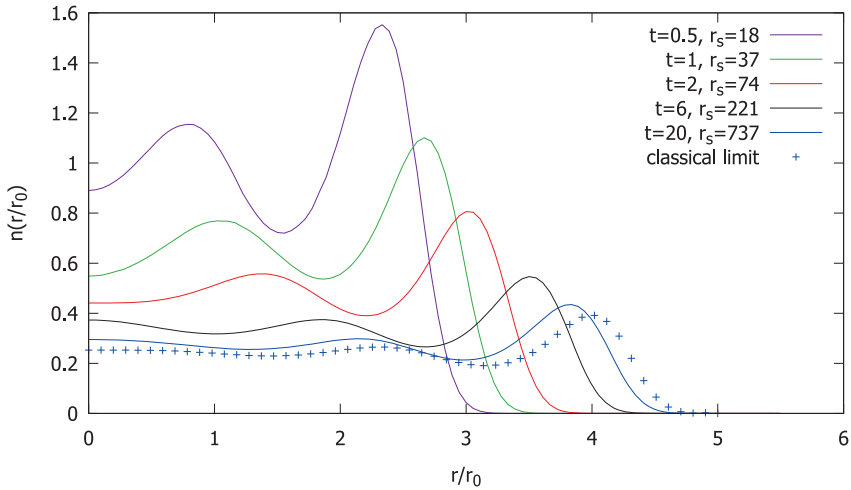

Fig. 11 Quantum effects for a trapped system of 100 particles. Here, $\Gamma = 20$ for all while the temperature parameter varies from $t = 0.5$ to $t = 20$.

potential. There is much more to be done with this classical description of a quantum system in the low t domain. At much smaller N, connection to other studies of quantum dots and ultracold gases should be useful. Other properties such as spin polarization, coherent control of trap properties, charge dependence, and others acceptable to direct observation can be addressed. A different direction for application of the results here is obtained by the replacement of the harmonic trap with a Coulomb potential to calculate the electron distribution about an ion. This is a solved problem of quantum chemistry, but its extension to a random configuration of ions is of intense current interest for warm, dense-matter applications, e.g., the electron density in the presence of an ion configuration. Such densities are required to compute the forces in quantum MD simulations for the ions in warm, dense matter at finite temperatures where traditional density functional methods fail (e.g., the traditional Kohn–Sham self-consistent equations for temperatures near the Fermi temperature). Here, those self-consistent equations are replaced with the classical integral equations of AHNC. This advantage has been stressed by Dharma-wardana.[24]

5. Discussion

The extreme conditions of long-range Coulomb charges, confined at strong coupling and finite temperatures, lead to complex structures: radial shell structure and broken symmetry angular ordering within the shells.

At the classical conditions, a density functional representation with strong coupling correlations from the OCP is able to capture quantitatively the transition from simple uniform filling at weak coupling to the formation of "atomic" shell structure. At infinite coupling, the ground state (ordered state) is closely related to the Thomson problem (sharp shell radii, no interactions between shells), extended here to finite temperature (e.g., like Debye–Waller broadening). The classical fluid phase with uniform angular distribution is now well studied by MC, MD, and theory—the features discussed in Ref. 9 are given quantitatively as a function of Γ, $\bar{N}$, e.g., number of shells, occupancy, amplitude, and location. The classical ordered phase also is well studied in the ground state, but less so at finite temperatures. The onset of localization within shells seems not to be sharp but rather gradual, as is the formation of shells, as a function of Γ (see however Refs. 25, 26 for some quantitative studies). The Thomson sites associated with the occupation number for a given shell provide a good reference for this localization, as confirmed by ground-state minimum energy models. The latter models, and simulation, indicated that there are metastable configurations with similar energy so the minimization requires care. It is possible that a more controlled limit is obtained from the limit of finite temperature studies as described here.

The quantum case is well studied at the ground state in the context of quantum dots, nanodevices, and related systems. The case of higher temperatures and transition to classical behavior is more limited, both from theory and simulation. The classical map method described here is particularly well suited for this domain, but has not been explored very much. Some of the advantages for states of warm, dense matter have been outlined in Ref. 24. Another interesting question is the line for Wigner crystallization (see Fig. 1), whose location is known only at $T = 0$ and in the high-temperature classical limit.

Acknowledgments

Much of the work summarized here was done in collaboration with the Bonitz group at Christian-Albrects University. The work of J.W. and J.D. was supported by US DOE Grant DE-SC0002139.

References

1. Thomson, J. J. On the Structure of the Atom. *Philos. Mag.* **1904**, 7, 237.
2. Pohl, T.; Pattard, T.; Rost, J. M. Coulomb Crystallization in Expanding Laser-Cooled Neutral Plasmas. *Phys. Rev. Lett.* **2004**, *92*, 155003.

3. Arp, O.; Block, D.; Piel, A.; Melzer, A. Dust Coulomb Balls: Three-Dimensional Plasma Crystals. *Phys. Rev. Lett.* **2004**, *93*, 165004; Arp, O.; Block, D.; Bonitz, M.; Fehske, H.; Golubnychiy, V.; Kosse, S.; Ludwig, P.; Melzer, A.; Piel, A. 3D Coulomb Balls: Experiment and Simulation. *J. Phys. Conf. Ser.* **2005**, *11*, 234.
4. Ludwig, P.; Kosse, S.; Bonitz, M. Structure of Spherical Three-Dimensional Coulomb Crystals. *Phys. Rev. E* **2005**, *71*, 046403.
5. Bonitz, M.; Block, D.; Arp, O.; Golubnychiy, V.; Baumgartner, H.; Ludwig, P.; Piel, A.; Filinov, A. Structural Properties of Screened Coulomb Balls. *Phys. Rev. Lett.* **2006**, *96*, 075001.
6. Golubnychiy, V.; Baumgartner, H.; Bonitz, M.; Filinov, A.; Fehske, H. Screened Coulomb Balls–Structural Properties and Melting Behaviour. *J. Phys. A Math. Gen.* **2006**, *39*, 4527.
7. Baumgartner, H.; Kählert, H.; Golubnychiy, V.; Henning, C.; Käding, S.; Melzer, A.; Bonitz, M. Structural and Dynamical Properties of Yukawa Balls. Contrib. *Plasma Phys.* **2007**, *47*, 281; Baumgartner, H.; Asmus, D.; Golubnychiy, V.; Ludwig, P.; Kählert, H.; Bonitz, M. Ground States of Finite Spherical Yukawa Crystals. *New J. Phys.* **2008**, *10*, 093019.
8. Cioslowski, J.; Grzebielucha, E. Parameter-Free Shell Model of Spherical Coulomb Crystals. *Phys. Rev. E* **2008**, *78*, 026416.
9. Wrighton, J.; Dufty, J. W.; Kählert, H.; Bonitz, M. Charge Correlations for Charges in a Harmonic Trap. *Phys. Rev. E* **2009**, *80*, 038912.
10. Wrighton, J.; Dufty, J. W.; Bonitz, M.; Kählert, H. Shell Structure of Confined Charges at Strong Coupling. *Contrib. Plasma Phys.* **2010**, *50*, 26.
11. Wrighton, J.; Kählert, H.; Ott, T.; Ludwig, P.; Thomsen, H.; Dufty, J.; Bonitz, M. Charge Correlations in a Harmonic Trap. *Contrib. Plasma Phys.* **2012**, *52*, 45.
12. Dufty, J. W.; Dutta, S. Classical Representation of a Quantum System at Equilibrium: Theory, Phys. Rev. E 87, 032101 (2013). *Contrib. Plasma Phys.* **2012**, *52*, 100.
13. Dutta, S.; Dufty, J. Classical Representation of a Quantum System at Equilibrium: Applications. *Phys. Rev. E* **2013**, *87*, 032102.
14. Dutta, S.; Dufty, J. Uniform Electron Gas at Warm, Dense Matter Conditions. *Euro. Phys. Lett.* **2013**, *102*, 67005.
15. Wrighton, J.; Dufty, J.; Dutta, S. Finite Temperature Quantum Effects in Many-Body Systems by Classical Methods. In Advances in Quantum Chemistry, Vol. 71; Elsevier: NY, 2015.
16. Wrighton, J.; Dufty, J.; Dutta, S. Finite-Temperature Quantum Effects on Confined Charges. *Phys. Rev. E* **2016**, *94*, 053208.
17. Dufty, J. W. Density Functional Theory for Electron Gas and for Jellium. *Langmuir* **2017**, *33* (42), 11570.
18. Silvestri, L. G.; Stanek, L. J.; Dharuman, G.; Choi, Y.; Murillo, M. S. Sarkas: A Fast Pure-Python Molecular Dynamics Suite for Plasma Physics. *Comput. Phys. Commun.* **2022**, *272*, 108245.
19. Sarkas., 2022. https://github.com/murillo-group/sarkas.
20. Hansen, J.-P.; MacDonald, I. *Theory of Simple Liquids*; Academic Press: San Diego, CA, 1990.
21. Ng, K. C. Hypernetted Chain Solutions for the Classical One-Component Plasma up to $\Gamma = 7000$. *J. Chem. Phys.* **1974**, *61*, 2680.
22. Thompson, A. P.; Aktulga, H. M.; Berger, R.; Bolintineanu, D. S.; Brown, W. M.; Crozier, P. S.; in 't Veld, P. J.; Kohlmeyer, A.; Moore, S. G.; Nguyen, T. D.; Shan, R.; Stevens, M. J.; Tranchida, J.; Trott, C.; Plimpton, S. J. LAMMPS–A Flexible Simulation Tool for Particle-Based Materials Modeling at the Atomic, Meso, and Continuum Scales. *Comput. Phys. Commun.* 2022, *271*, 10817.
23. LAMMPS., 2022. http://lammps.org.

24. Dharma-wardana, M. W. C. A Review of Studies on Strongly-Coupled Coulomb Systems Since the Rise of DFT and SCCS-1977. *Contrib. Plasma Phys.* **2015**, *55*, 85; Dharma-wardana, M. W. C. Current Issues in Finite-T Density-Functional Theory and Warm-Correlated Matter. *Computation* **2016**, *4*, 16.
25. Kählert, H.; Bonitz, M. How Spherical Plasma Crystals Form. *Phys. Rev. Lett.* **2010**, *104*, 015001.
26. Galván-Moya, J. E.; Altantzis, T.; Nelissen, K.; Peeters, F.; Grzelczak, M.; Liz-Marzán, L. M.; Bals, S.; Van Tendeloo, G. Self-Organization of Highly Symmetric Nanoassemblies: A Matter of Competition. *ACS Nano* **2014**, *8*, 3869.